Article

Hollow Silica Spheres: Synthesis and Mechanical Properties

Lijuan Zhang, Maria D'Acunzi, Michael Kappl, Gu#nter K. Auernhammer, Doris Vollmer, Carlos M. van Kats, and Alfons van Blaaderen

Langmuir, **2009**, 25 (5), 2711-2717• DOI: 10.1021/la803546r • Publication Date (Web): 27 January 2009

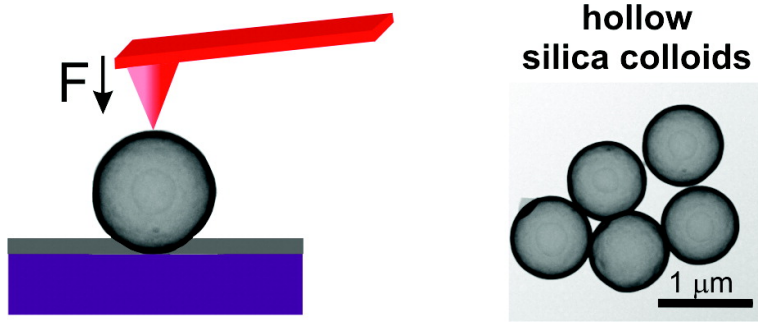

More About This Article

Additional resources and features associated with this article are available within the HTML version:

- Supporting Information
- Access to high resolution figures
- Links to articles and content related to this article
- Copyright permission to reproduce figures and/or text from this article

View the Full Text HTML

Hollow Silica Spheres: Synthesis and Mechanical Properties

Lijuan Zhang, Maria D'Acunzi, Michael Kappl, Günter K. Auernhammer, and Doris Vollmer*

Max Planck Institute for Polymer Research, Ackermannweg 10, 55128 Mainz, Germany

Carlos M. van Kats and Alfons van Blaaderen

Soft Condensed Matter, Debye Institute for Nanomaterials Science, Utrecht University, Princetonplein 5, 3584 CC Utrecht, The Netherlands

Received October 24, 2008. Revised Manuscript Received December 16, 2008

Core−shell polystyrene−silica spheres with diameters of 800 nm and 1.9 μm were synthesized by soap-free emulsion and dispersion polymerization of the polystyrene core, respectively. The polystyrene spheres were used as templates for the synthesis of silica shells of tunable thickness employing the Stöber method [Graf et al. *Langmuir* **2003**, *19*, 6693]. The polystyrene template was removed by thermal decomposition at 500 °C, resulting in smooth silica shells of well-defined thickness (15−70 nm). The elastic response of these hollow spheres was probed by atomic force microscopy (AFM). A point load was applied to the particle surface through a sharp AFM tip, and successively increased until the shell broke. In agreement with the predictions of shell theory, for small deformations the deformation increased linearly with applied force. The Young's modulus (18 ± 6 GPa) was about 4 times smaller than that of fused silica [Adachi and Sakka *J. Mater. Sci.* **1990**, *25*, 4732] but identical to that of bulk silica spheres (800 nm) synthesized by the Stöber method, indicating that it yields silica of lower density. The minimum force needed to irreversibly deform (buckle) the shell increased quadratically with shell thickness.

I. Introduction

Silica particles are chemically inert and can be easily modified from hydrophilic to hydrophobic by simple chemical reactions.[3] Nevertheless, fast sedimentation due to their high density prevents homogeneous dispersion of silica particles in many liquids without continuous stirring for particles larger than several hundred nanometers. This disadvantage can be overcome using core−shell polystyrene (PS)−silica particles. PS cores allow matching of the density of the hybrid particles. Furthermore, removing the PS core would result in hollow silica particles, i.e. silica capsules. Silica shells are salt and pH insensitive, i.e., they do not disintegrate, and are nontoxic. However, it is difficult to obtain micro- or even submicrometer-sized silica spheres with thin, intact porous shells,[4] and only a few strategies have been proven suitable to yield well-defined silica shells.[5−10] Intact porous shells can easily be achieved by fabricating hollow polymer particles, i.e., polymer capsules.[4,11−15] Here the porosity can be tuned by pH.[13] These techniques have been applied in the encapsulation of flavors, fragrances, or pharmaceutical agents as well as in the coating of textiles or paper.[16] Polymer capsules served as a model system to show that atomic force microscopy (AFM) is a suitable technique to determine the elastic modulus of such thin shells.[14,17,18] The mechanical properties are important, as they govern the stability of the hollow particles to external forces. By combining AFM and reflection interference contrast microscopy, different deformation regimes could be distinguished: a small deformation, an irreversible buckling regime, and the rupturing of the capsules. In the small deformation regime, the stiffness of the capsules increases with the square of the shell thickness.[17] The elastic modulus of most polymer capsules is on the order of a few hundred megapascals.[14,17] The stability and handling of the capsules, however, would be substantially improved by a larger elastic modulus as would be expected for hollow silica spheres. Hollow silica particles are also promising systems as drug delivery vehicles.[19−21]

We have developed a procedure to prepare monodisperse hollow silica spheres of well-defined and tuneable thickness, using PS particles as templates. Small PS spheres (< 1 μm) used as templates were synthesized by soap-free emulsion polym-

* Corresponding author. Electronic address: vollmerd@mpip-mainz.mpg.de.

(1) Graf, C.; Vossen, D. L. J.; Imhof, A.; van Blaaderen, A. *Langmuir* **2003**, *19*, 6693.
(2) Adachi, T.; Sakka, S. *J. Mater. Sci.* **1990**, *25*, 4732.
(3) van Helden, A. K.; Jansen, J. W.; Vrij, A. *J. Colloid Interface Sci.* **1981**, *81*, 354.
(4) Caruso, F.; Caruso, R. A.; Möhwald, H. *Science* **1998**, *282*, 1111.
(5) Deng, Z.; Chen, M.; Zhou, S.; You, B.; Wu, L. M. *Langmuir* **2006**, *22*, 6403.
(6) Sacanna, S.; Rossi, L.; Kuipers, B. W. M.; Philipse, A. P. *Langmuir* **2006**, *22*, 1822.
(7) Zoldesi, C. I.; Steegstra, P.; Imhof, A. *J. Colloid Interface Sci.* **2007**, *308*, 121.
(8) Cheng, X. J.; Chen, M.; Wu, L. M.; You, B. *J. Polym. Sci., Part A: Polym. Chem.* **2007**, *45*, 3431.
(9) Peng, B.; Chen, M.; Zhou, S. X.; Wu, L. M.; Ma, X. H. *J. Colloid Interface Sci.* **2008**, *321*, 67.
(10) Zhang, T. R.; Ge, J. P.; Hu, Y. X.; Zhang, Q.; Aloni, S.; Yin, Y. D. *Angew. Chem., Int. Ed.* **2008**, *47*, 5806.
(11) Emmerich, O.; Hugenberg, N.; Schmidt, M.; Sheiko, S. S.; Baumann, F.; Deubzer, B.; Weis, J.; Ebenhoch, J. *Adv. Mater.* **1999**, *11*, 1299.
(12) Jungmann, N.; Schmidt, M.; Maskos, M.; Weis, J.; Ebenhoch, J. *Macromolecules* **2002**, *35*, 6851.
(13) Heuvingh, J.; Zappa, M.; Fery, A. *Langmuir* **2005**, *21*, 3165.
(14) Dubreuil, F.; Elsner, N.; Fery, A. *Eur. Phys. J. E* **2003**, *12*, 215.
(15) Donath, E.; Sukhorukov, G. B.; Caruso, F.; Davis, S. A.; Möhwald, H. *Angew. Chem., Int. Ed.* **1998**, *37*, 2201.
(16) Wilkox, D. L.; Berg, M.; Bernat, T.; Kellerman, D.; Cochran, J. K., Jr. Hollow and solid spheres and microspheres: Science and technology associated with their fabrication and application. In *Materials Research Society Proceedings*; Materials Research Society: Pittsburgh, PA, 1995; Vol. *372*.
(17) Fery, A.; Weinkamer, R. *Polymer* **2007**, *48*, 7221.
(18) Vinogradova, O. I. *J. Phys.: Condens. Matter* **2004**, *32*, 1105.
(19) Luo, D.; Pullela, S. R.; Marquez, M.; Cheng, Z. *Biomicrofluidics* **2007**, *1*, 034102.
(20) Yang, J.; Lee, J.; Kang, J.; Lee, K.; Suh, J.-S.; Yoon, H.-G.; Huh, Y.-M.; Haam, S. *Langmuir* **2008**, *24*, 3417.
(21) Clifford, N. W.; Swaminathan, K.; Raston, C. L. *J. Mater. Chem.* **2008**, *18*, 162.

10.1021/la803546r CCC: $40.75
Published on Web 01/27/2009

Table 1. Details of the Synthesis of PS Spheres Obtained via Soap Free Emulsion Polymerization

	amounts in grams
styrene	25
divinylbenzene	0.25
acrylic acid	0.15
ammonium persulfate	0.11
Milli-Q water	300

Table 2. Details of the Synthesis of PS Spheres Obtained via Dispersion Polymerization

	amounts in grams	
	1st step	2nd step
styrene	6.4+ 2.7	1.27
PS spheres		6.4
acrylic acid		1.05
poly(acrylic acid)	0.5	
azobisisobutyronitrile	0.200	0.06
Milli-Q water	5	50
ethanol	67 + 2.4	39.5

erization, and larger ones were formed by dispersion polymerization (a few μm). We obtained closed intact shells even with silica layers as thin as 15 nm. Whereas such thin shells are quite floppy, the stiffness of the shells increases with shell thickness. The thickness can be easily and sensitively tuned by composition. Surprisingly, the shell thickness hardly influenced the elastic modulus, implying that even a 15 nm thick shell behaves like bulk Stöber silica. Because of the lower density of silica spheres synthesized by the Stöber method, which is caused by an incomplete level of condensation, these spheres have a significantly lower elastic modulus than fused silica.

II. Experiment

A. Materials. Styrene was purchased from Acros Organics (99% extra pure, stabilized). The inhibitor was removed from the styrene by washing three times with 2 M sodium hydroxide solution and three times with Milli-Q water. The washed styrene was distilled under reduced pressure before use. (3-Aminopropyl)triethoxysilane (Aldrich, 99%) was distilled before use. All other chemicals were used without further purification: sodium hydroxide (WTL Laborbedarf GmbH, 99%), divinylbenzene (Fluka, mixture of isomers $\approx$ 80%), ammonium persulfate (Acros Organics, 98%), acrylic acid (Acros Organics, 99.5%, stabilized), absolute ethanol (Sigma Aldrich), poly(allylamine hydrochloride) (PAH, Aldrich, average $M_w \approx 15\,000$ g/mol), polyvinylpyrrolidone (PVP, Fluka, K 90, $M_w \approx 360\,000$ g/mol), ammonia (Fluka, 25 wt % in water), and tetraethoxysilane (TES) (Acros Organics, 98%). Milli-Q water was obtained from a Millipore purification system operating at 18.2 MΩ cm. It was distilled before use. For the spheres synthesized by dispersion polymerization, azobisisobutyronitrile (Fluka, 98%) and poly(acrylic acid) (Sigma Aldrich), $M_w \approx 450\,000$ g/mol) were used.

B. Emulsion Polymerization of Styrene Colloids. Soap-free emulsion polymerization was carried out in 500 mL three-necked flasks equipped with a condenser, a PTFE stirrer, and a gas inlet. Milli-Q water was put in the reactor, and nitrogen was bubbled for 20 min. Ammonium persulfate was added to the water, and the system was heated to 75 °C. A mixture of divinylbenzene, acrylic acid, and styrene was added dropwise within 1 h (see Table 1 for the details of the preparations). Thereafter, an aliquot of ~1 mL was taken and imaged by scanning electron microscopy (SEM). Samples (labeled as PSE) were cleaned by centrifugation in water and ethanol at least six times.

C. Dispersion Polymerization of Styrene Colloids. Dispersion polymerization is well suited to obtain micrometer-sized PS spheres. These were synthesized according to the following procedure: in a 250 mL three-necked flask equipped with a condenser, a mixture of poly(acrylic acid), part of the styrene (6.4 g) and ethanol (67 g), and Milli-Q water (amounts listed in Table 2, first step) were mixed and flushed with nitrogen for 15 min. Then the system was closed and heated to 70 °C. When the temperature was stable, a mixture of the remaining styrene (2.7 g), azobisisobutyronitrile, and ethanol was added. The reaction was allowed to proceed for 20 h. For subsequent silica coating, the surface of the spheres was functionalized with poly(acrylic acid-*co*-styrene), necessary for coating with PAH. The functionalization procedure is similar to the one reported in ref 22. PS spheres were washed and dispersed in ethanol. Then the same volume of water was added (amounts listed in Table 2, second step). A mixture of styrene, azobisisobutyronitrile and acrylic acid was added to the dispersion, and the mixture was stirred for 20 h. After being deoxygenated by nitrogen flow for 20 min, the system was closed and heated to 75 °C for about 20 h. Samples (labeled as PSD) were cleaned by centrifugation in water and ethanol at least six times.

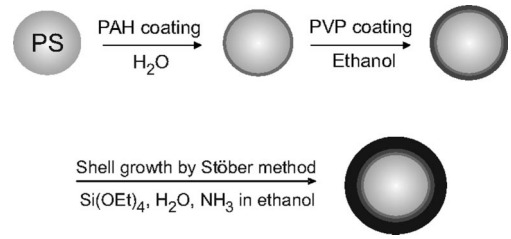

Figure 1. Schematic representation of the reaction scheme to coat PS spheres with silica.

D. Synthesis of Bulk Silica Spheres. Bulk silica spheres were synthesized according to the Stöber procedure:[23,24] 67 mL of ethanol and 5 mL of ammonia (25% w/w) were put in a 500 mL flask. After adding 0. 01 g of (3-amino-propyl)triethoxysilane (APS) and 3 mL of TES dropwise, the mixture was left under stirring overnight. After that, 25 mL of TES and 20 mL of water were added simultaneously within 24 h. According to our SEM images, silica spheres with a diameter of 400 nm were obtained. In order to increase the size of the spheres, the following step was repeated three times: 25 mL of TES, 0.01 g of APS, 20 mL of water, and 1.55 mL of ammonia were added to the reaction mixture and kept under stirring for 24 h. After the last step, the reaction mixture was washed six times with fresh ethanol. According to SEM, the size of the spheres increased to 720 ± 30 nm.

E. Synthesis of Silica Shells. For uniform shells, smooth and spherical cores are required. Therefore, prior to shell synthesis we determined the shape of the core particles under vacuum. After 24 h of reaction time, the particles appeared smooth in the SEM images.

To facilitate the formation of silica shells on the PS spheres, we pretreated the PS spheres with polyelectrolytes (see Figure 1). The PS spheres were dispersed in water (concentration of 68 g/L). A 10 mL solution of PAH dispersed in water and sodium chloride (NaCl) was prepared ($c = 1.2$ g/L in PAH and 1.4 g/L in NaCl). The further procedure was according to that outlined in ref 1. A 4 mL portion of the colloidal dispersion was added dropwise under stirring. This dispersion was stirred for 1 h and then centrifuged, washed twice with fresh water, and finally redispersed in a solution of PVP in ethanol ($c = 7$ g/L). After another 1 h of stirring, the sample was centrifuged twice and redispersed in 20 mL fresh ethanol. To form the silica shell, ammonia (1.6 mL) and different amounts of TES (amounts listed in Table 3) were added. The spheres were washed three times in fresh ethanol.

F. Preparation of Hollow Silica Spheres. Core−shell PS−silica spheres were stored in ethanol. In order to prepare hollow spheres, a sample was dried and kept at 500 °C in air for 3.5 h in a furnace. The condensed spheres could be redispersed in ethanol as single particles, as indicated by the fact that the redispersed systems could still form large colloidal crystals (results not shown).

G. Characterization. SEM (LEO 1530 Gemini, Oberkochen, Germany) was used to characterize colloids in terms of sphere size

(22) Tuncel, A.; Kahraman, R.; Piskin, E. *J. Appl. Polym. Sci.* **1994**, *51*, 1485.
(23) Verhaegh, N. A. M.; van Blaaderen, A. *Langmuir* **1994**, *10*, 1427.
(24) Stöber, W.; Fink, A.; Bohn, E. *J. Colloid Interface Sci.* **1968**, *26*, 62.
(25) Butt, H.-J.; Jaschke, M. *Nanotechnology* **1995**, *6*, 1.

Table 3. Core−Shell PS−Silica Spheres of Well-Defined Shell Thickness[a]

PS sample	diameter (nm)[b]	TES (mL)	shell thickness (nm)
PSE	790 ± 70	0.10	15
PSE	790 ± 70	0.20	23[c]
PSE	790 ± 70	0.30	37[c]
PSD	1870 ± 60	0.12	30
PSD	1870 ± 60	0.24	50[d]
PSD	1870 ± 60	0.30	70[d]

[a] PSE stands for PS spheres synthesized by soap-free emulsion polymerization. The larger spheres, denoted as PSD, were synthesized by dispersion polymerization. The PS spheres were coated with a silica shell of varying thickness depending on the amount of TES (see Figure 1). [b] Sphere diameter according to SEM, average of ∼100 particles. [c] Shell thickness according to TEM. [d] Shell thickness according to SEM taking the difference between the diameter before and after coating.

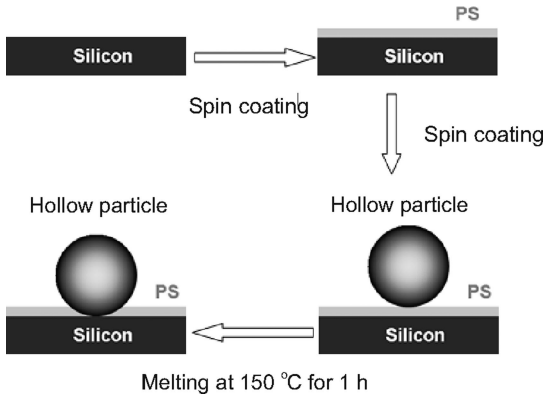

Figure 2. Schematic representation of the procedure taken to immobilize the spheres on the substrate.

and surface roughness. Samples were prepared by evaporation of a small droplet of a dilute dispersion of spheres in water or ethanol on a silicon substrate. Hollow silica spheres were also imaged by a transmission electron microscope (TEM, Tecnai F20, FEI; 200 kV) to measure the shell thickness.

H. Preparation of Samples for AFM Measurements. The elastic modulus of the bulk and hollow silica spheres were determined by AFM force spectroscopy. To prevent the spheres from shifting or rolling on the substrate during measurements, they were partially embedded in a thin PS film (5.0 mg/mL, M_w = 130 000 g/mol dissolved in toluene) obtained by spin coating (Delta 80 μ_B, Süss MicroTec Laboratory Equipment GMBH, Germany, 1000 rpm for 60 s) (see Figure 2). Hollow silica spheres dispersed in ethanol were deposited onto the glassy PS film by spin coating (2000 rpm for 60 s) of the dispersion. The substrates were placed in an oven and kept at 150 °C for about 1 h. The melting of the film causes capillary forces that suck the spheres into the film and lead to a strong fixation onto the substrate. After cooling down to room temperature, the thickness of the PS films was measured using a surface profiler (KLA Tencor, LOT-Oriel GmbH & Co. KG, Germany) and was found to range between 55 and 75 nm depending on position.

I. AFM Imaging and Force Measurements. Tapping-mode AFM imaging and force measurements were performed with a MultiMode Nanoscope IIIa SPM from Digital Instruments (Veeco Metrology Group, Plainview, NY) at 25 ± 2 °C using silicon AFM probes (OMCL-AC 160TS, Olympus, Japan) with a resonance frequency of about 300 kHz and a tip radius of less than 20 nm. The spring constants of the cantilevers were determined by the thermal noise method, as described in ref 25. They were found to be 42 ± 12 N/m. For each experiment, a fresh silicon substrate and one of the samples were mounted on the same AFM specimen holder. Before starting the force measurements, the immobilized silica spheres were imaged in tapping mode, and a well-shaped sphere was chosen. By repeatedly zooming in, we carefully located the top of the target sphere. For the ensuing force measurements, the substrate was periodically moved up and down at a constant scan rate (1.0 Hz) while the cantilever deflection was measured. The result is a graph of the cantilever deflection signal in volts versus the height position of the scanner. For each of these measurements on the spheres, about 60 reference curves were recorded on the bare silicon substrate to obtain the deflection sensitivity, i.e., the conversion factor between the measured deflection signal in volts and the actual cantilever deflection in nanometers. Recording the deflection sensitivity before and after sphere experiments allowed us to exclude that changes in the deflection sensitivity occurred during measurements. Force versus distance curves were calculated from the deflection versus piezo position curves by multiplying the cantilever deflection with the spring constant to obtain the force and subtracting the cantilever deflection from the height position to obtain the distance. Zero distance was derived from the linear contact part of force curves as described previously.[26] Within a series of force measurements, the maximum cantilever deflection was increased step by step, corresponding to increasingly higher force loads on the spheres. For each particle and each fixed load, typically 30 force curves were recorded.

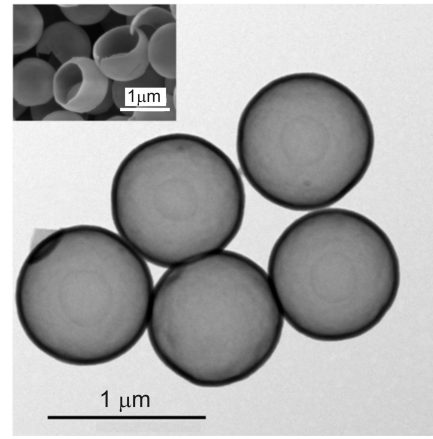

Figure 3. TEM image of hollow silica spheres with a diameter of 790 nm (sample PSE) and a shell thickness of 37 nm. Inset: Occasionally broken shells were found. SEM image of several broken shells.

III. Results

A. Synthesis of Hollow Silica Spheres by Templating. Smooth silica shells were obtained after pretreating the PS template particles with a polyelectrolyte (PAH) to induce a positively charged surface, as described in detail in section II. After this additional step, shell synthesis applying the Stöber method yielded shell thicknesses of 15−70 nm (Table 3) depending on experimental conditions, in particular on the amount of TES.

Even after thermal decomposition of the PS template, the silica shells remained intact and smooth, as demonstrated by SEM or TEM. In the TEM picture shown in Figure 3, the particles appear translucent, and the shell thickness is given by the width of the dark rims. There were hardly any variations in shell thickness, and no evidence of PS remnants was found. The inset of Figure 3 shows some fragmented and deformed spheres to visualize the thin shells and hollow interior, but damaged shells were in fact a rare finding.

B. AFM Imaging. Before investigating the elastic response of the hollow silica spheres, we imaged the particles. In AFM images, the hollow spheres always appeared slightly larger and less spherical (Figure 4A) than in TEM, (Figure 3). This is a typical artifact from the convolution between the tip shape and the actual shape of the sphere. Zooming in on the top of the sphere allowed us to determine the surface roughness of the spheres. Figure 4B is a phase image of the top of a sphere that

(26) Butt, H.-J.; Cappella, B.; Kappl, M. *Surf. Sci. Rep.* **2005**, *59*, 1.

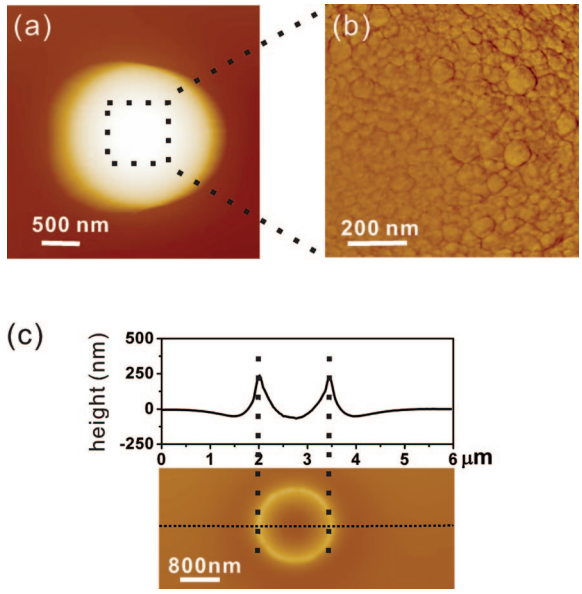

Figure 4. AFM height image of a hollow silica sphere with a diameter of 1.9 μm and a shell thickness of 50 nm (a) and a zoom in on the top of the sphere (b). The shell has a roughness of about 2.5 ± 0.5 nm. (c) Section analysis and an image of the groove formed after the sphere was removed. The depth of the groove h_{groove} is about 67 nm, which is close to the thickness of the PS film, $h_{PS} \approx 69$ nm, determined using a surface profiler.

shows the surface structure. Surface roughness was determined from height images by flattening the sphere top area (400 × 400 nm^2) and calculating the root-mean-square (rms) roughness. The shells grown on PS spheres synthesized by dispersion polymerization had a roughness of about 2.5 ± 0.5 nm, whereas the shells grown on PS synthesized by soap-free-emulsion polymerization had a surface roughness of only 1.6 ± 0.2 nm. In both cases, the shell seemed to consist of small silica particles merged together.

For the analysis of the force measurements, it is important to know whether the measured deformation originates only from deformation of the shells and not from deformation of the spin-coated PS film. If the immobilized spheres are separated from the silicon substrate by a thick PS layer, deformation of the softer PS film upon applying a point load to the top of the sphere might contribute substantially to the measured deformation. To check the thickness of the PS layer remaining underneath the spheres, we sheared off several spheres using a line scan of the AFM tip and imaged the resulting surface dimple. Figure 4C shows a height image (bottom) and cross section (top) along the dotted line. The bridge-like height profile shows the thickness variation of the PS film with respect to the thickness of the undistorted PS film (height ≡ 0). When approaching the groove from either side, the relative height levels first decrease by a few nanometers, then increase strongly, pass a maximum, and meet at negative values. The height of the PS ring depends on the wetting behavior of the silica-coated spheres toward PS. The difference between (i) the thickness of the PS film as determined by the surface profiler h_{PS} and the groove depth h_{groove} yields the height of the residual PS layer Δh_{PS}. According to this analysis, only a few nanometers of the PS film ($\Delta h_{PS} \approx 2-5$ nm) remain between the sphere and the substrate.

The contact area of the cup S_{cup} can be estimated from the radius and the contact height $S_{cup} = \pi h_{PS}(4R - h_{PS}) \approx 4\pi h_{PS}R$, where R stands for the radius of the sphere. As contact area we consider only the groove, as the PS film should have a larger elastic modulus compared to the PS forming the ring.

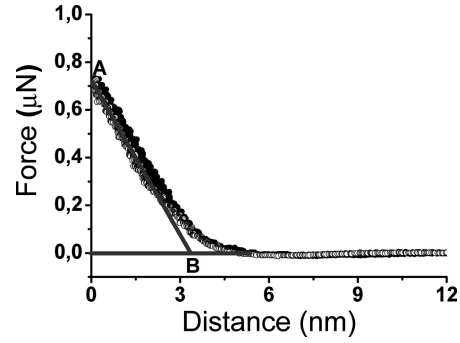

Figure 5. A typical force curve of a hollow silica sphere with a shell of 50 nm and a diameter of 1.9 μm, sample PSD. The open spheres denote the approach, and the filled spheres denote the retract part of the curve. Hardly any hysteresis is visible, i.e., the deformation is elastic.

To decide whether the force on the PS film is sufficient to compress the PS film, the forces per unit area need to be compared. This is proportional to the ratio between the contact area between the tip and the shell S_{tip} and S_{cup}.

$$\frac{S_{tip}}{S_{cup}} \approx \frac{h_{tip}R_{tip}}{h_{PS}R} \quad (1)$$

where R_{tip} stands for the tip radius, and h_{tip} is the deformation of the shell induced by the tip. If $h_{tip} < h_{PS}$, the deformation of the PS film is negligible, as $S_{tip}/S_{cup} > 10$.

C. Force versus Deformation. Force versus distance curves on hollow silica spheres are obtained by applying a point load on their top with the AFM tip (Figure 5). At large distances, the force is zero, as the tip does not touch the sphere. When tip and sphere start to come into contact, the sphere starts to deform. We observed a transition region of about 1 nm width where the relation between force and deformation was nonlinear. After this regime, further approach led to a strong linear increase of the force. We used a fit of this linear part for evaluating the elastic properties and determining the distance for zero deformation.

To obtain a force−deformation curve, for each force−distance curve we determined the deformation at maximum applied force F_{max}. F_{max} is given by the intersection of the linear extrapolation of the force versus distance curve with the force axis (A in Figure 5). The corresponding deformation was determined from the intersection of the linear fit with the linear extrapolation of the zero deformation line (B in Figure 5). From each such force−distance curve, one obtains a single data point (B, A) for the corresponding force versus deformation dependence. About 30 force curves were recorded for each maximum applied force. From taking force curves at different defined maximum forces, we obtained the dependence of the deformation on the applied force shown in Figure 6.

The plot shows a linear increase of force F_{max} with deformation for deformations of up to 30 nm. The clustering of the data points in Figure 6 arises from the way in which the data were acquired: The vertical spread (in force) results mainly from variations in how precisely the trigger function of the AFM piezo movement was reversible. The lateral spread (in deformation) gives the experimental error for each fixed load. It may be due to slight lateral variations of the shell thickness, as the position may change by a few nanometers while recording the force curves. The inset in Figure 6 gives the force versus deformation curve for a single measurement as obtained from the force versus distance curves. This supports the linear dependence of the deformation on the force for small deformations. For deformations much smaller

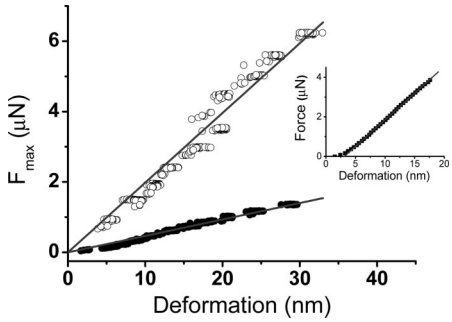

Figure 6. The deformation of the shell increases linearly with maximum loading force, F_{max}. Filled circles: Sample PSE, 800 nm sized hollow silica spheres with a shell of 23 nm. Open circles: Sample PSD, 1.9 μm sized hollow silica spheres with a shell of 70 nm. The gray lines show the fit through the data points. Inset: The force versus deformation curves are obtained from the approaching force versus distance curve in Figure 5. Solid line: linearly extrapolated force curve; open circles: experimental data points, sample PSD, with a shell thickness of 70 nm.

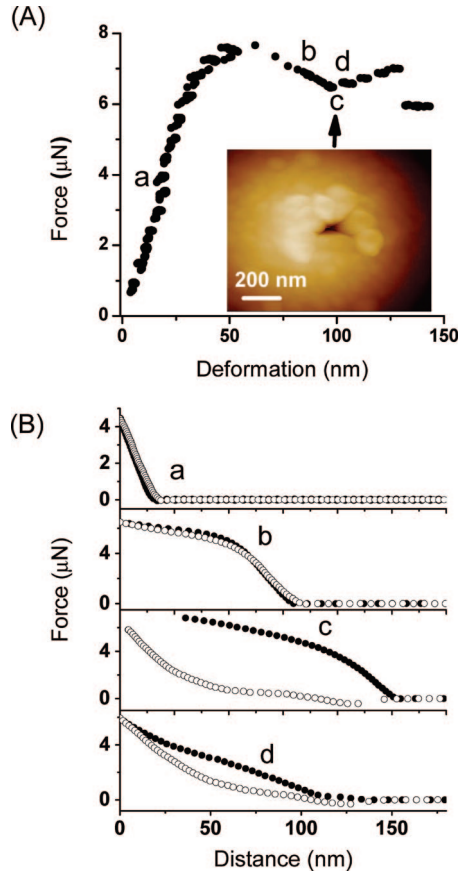

Figure 7. (A) Deformation of a single hollow silica sphere under increasing cantilever deflection (Sample PSD: 1.9 μm sized silica capsule with a shell thickness of 70 nm). Inset: AFM image taken after the approach curve showed a jump in. The dark spot in the middle of the sphere represents a hole in the shell. (B) Force versus distance curves recorded at different cantilever deflections. The approaching (filled circles) and retracting (open circles) curves shown in a−d correspond to points a−d in panel A.

than the shell thickness (Figure 7(A)a), the approaching and retracting curves are almost congruent and linear, indicating a fully reversible/elastic behavior (Figure 7(B)a). For larger deformations, the linear dependence of the deformation on the applied load breaks down (Figure 7(B)b), indicating the onset of shell buckling (apparent from the negative slope in the force curves) and plastic deformation. This is also reflected in the

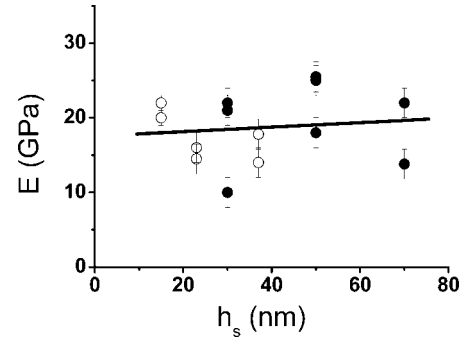

Figure 8. The Young's modulus E hardly depends on shell thickness h_s. Solid line: linear fit through the data points. Hollow circles: sample PSE; filled circles: sample PSD.

corresponding force versus distance curves, where buckling leads to a bending of the force curve at higher loading forces, while the approaching and retracting curves do still overlap (Figure 7(B)b).

Only at even higher forces do the approaching and retracting curves start to exhibit significant hysteresis, which is indicative of irreversible plastic deformation of the shells (Figure 7(B)c). An AFM image of the shell surface taken at this point (inset) shows a hole in the shell. As the depth of the hole (∼110 nm) exceeds the shell thickness (70 nm), it is likely the shell has been pierced. This is supported by the jump-in during the approach curve with a distance of 30 nm. After this damage, further increase of the loading force enlarges the hole and leads to pronounced hysteresis between the approaching and retracting curves (Figure 7(B)d).

D. Elastic Response. At small deformations, i.e., as long as the reversible deformation increases linearly with the loading force, the Young's modulus E is given by the thin shell model:[17,27−29] The ratio between shell thickness and radius is smaller than ∼1/10.[29]

$$E = \frac{\sqrt{3(1-\nu 2)}}{4}\frac{FR}{dh_s^2} \tag{2}$$

where d stands for the deformation, h_s is the shell thickness, R is the radius of sphere, F is the loading force, and ν is the Poisson ratio. Assuming the Poisson ratio to be $\nu = 0.17$,[2] eq 2 reads

$$E = 0.43\frac{FR}{dh_s^2} \tag{3}$$

Under these assumptions, the Young's modulus of our hollow spheres was found to be about 18 ± 6 GPa (Figure 8), irrespective of shell thickness and particle size. However, the measured value for the elastic modulus is four times smaller than that for fused silica, E = 76 GPa.[2]

Figure 9 shows the force−deformation curves for bulk silica spheres, before and after heating the spheres at 850 °C for five hours. After heating, the slopes of the force versus deformation curves are steeper by a factor of 4. As the slope is proportional to the elastic modulus, this suggests that the elastic modulus has increased equally. Unfortunately, absolute values of E for the bulk spheres cannot be determined since, in bulk spheres, the elastic modulus is given by the Oliver-Pharr model of nanoindentation. This, however, requires knowledge of the precise shape

(27) Koiter, W. T. *A Spherical Shell under Point Loads at Its Poles*; Macmillan: New York, 1963.
(28) Reissner, E. *J. Math. Phys.* **1949**, *25*, 279.
(29) Wan, F. Y. M.; Douglas Gregory, R.; Milac, T. I. *SIAM J. Appl. Math.* **1999**, *59*, 1080.

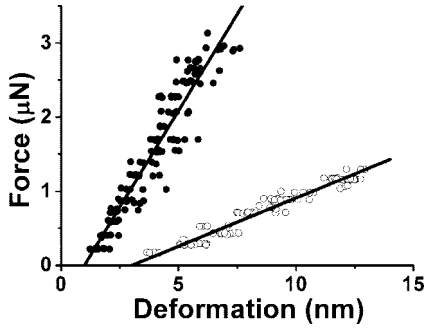

Figure 9. Dependence of the deformation on the loading force for bulk silica spheres. Heating the spheres at 850 °C for 5 h increases the stiffness of the spheres. The diameters of the bulk silica spheres were 790 ± 25 nm before heating the sphere and shrank to 720 ± 25 nm after heating. The solid lines show the result of a linear least-squares fit through the data points. Open circles: before heating; filled circles: after heating.

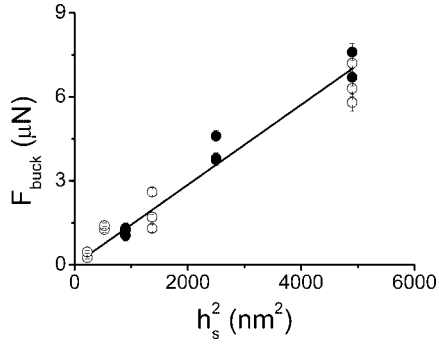

Figure 10. Dependence of the buckling force F_{buck} on the shell thickness h_s^2. A least-squares fit (solid line) supports a parabolic increase of F_{buck} with h_s^2. Open circles: sample PSE; filled circles: sample PSD.

of the last few nanometers of the AFM tip, which we do not have.[30]

Heating also induced shrinkage of the spheres by a factor of 1.35 ± 0.1. Thus, the Stöber synthesized particles have a density close to 1.9−2.0 g/m as the particles contain water, ethoxy groups, and silanol groups. Still, its density is significantly below that of fused silica, i.e., 2.2 g/mL.[2]

Finally, we determined the typical loading force for the onset of irreversible buckling, F_{buck}. As the buckling transition is not sharply defined (deviation of the linear regime in the force versus distance curves, Figure 7B), we took the maximum in the force−deformation curve (Figure 7A). It increases with shell thickness (Figure 10) but does not depend on the sphere diameter in the accessible size range. For shell thicknesses smaller than 15 nm, the shells are so fragile that buckling or rupturing is easily induced by capillary forces while drying or imaging the capsules. In thick shells, the force needed to induce buckling is so large that F_{buck} may be influenced by damage to the AFM tip. These measurements should be performed with a blunter tip.

IV. Discussion

In the present work, we synthesized hollow silica particles whose size could be tuned by the diameter of the PS core particles used as templates. In order to have a smooth shell, the surface of the PS core of positively charged PS particles proved suitable. In this way it is possible to take advantage of the electrostatic attraction of the PS surface with the negatively charged surface of silica particles. Since the PS particles obtained by emulsion polymerization are negatively charged, we reversed the charge by PAH coating. In the case of particles synthesized by dispersion polymerization, the surface of the particles had to be functionalized with poly(acrylic acid-*co*-styrene) in order to have negatively charged surface suitable for PAH coating. Unfunctionalized particles gave rise to silica shells with rough surfaces. We were able to obtain silica shells of predictable thickness. These shells retained their spherical shape after burning the PS core. Because the particles synthesized by emulsion polymerization are slightly cross-linked, the PS cores cannot be washed out in organic solvents. Therefore, the PS cores were burned instead of dissolved in an organic solvent. Furthermore, burning guarantees that even hollow particles with thick shells are PS free. Since many possible applications of hollow spheres imply mechanical stress, we determined the mechanical properties of individual spheres embedded in a polymer film by AFM. In SEM, thin shells (≤15 nm) appear quite floppy and may show dints. However, even for ≥15 nm shells, the resulting purely elastic response is independent of shell thickness and sphere size according to our measurements as long as the deformation is small compared to the sphere radius. However, heating the hollow spheres to 500 °C will decrease the number of unreacted silanol groups, causing the elastic modulus to increase. The Young's modulus was calculated applying the thin shell model. Under this assumption, even the thinnest shells ($h_s = 15 \pm 2$ nm) exhibit the same elastic behavior as bulk Stöber silica (Figure 8). This implies that shells comprising only about 100 layers of silica atoms behave as bulk silica. However, the Young's modulus of both hollow and solid silica spheres was about four times smaller than that of fused silica. To reproduce the conditions of fused silica production, we heat-treated our hollow spheres at 850 °C for several hours. After this treatment, the elastic modulus was similar to that of fused silica (Figure 9). This indicates that silica synthesized by the Stöber method contains a substantial number of silanol groups that are known to be transformed into Si−Si bonds by heating. This gives rise to an increase of the elastic modulus, as E increases with the number of siloxane bonds as they form a 3D structure.

The reason for the nonlinear onset in the force−distance curves when tip and sphere start to come into contact (Figure 6) is not clear. Since the approaching (open spheres) and retracting curves (filled spheres) are almost identical, the deformation is elastic, and no major adhesion forces are detected. The distance at which it occurs is in the same order as the surface roughness of the hollow shell, suggesting that, in this range, the shell cannot be considered as smooth.

At higher force loads, the linear elastic response changes to a flatter slope (Figure 7A, between a and b), indicating reversible indentation crossing over to buckling. In our experiments, the force maximum in the force−distance curve (Figure 6) was taken as the onset of irreversible buckling deformation. However, we could not determine the exact onset of irreversible buckling deformation. In our hollow particles, the buckling force increases with the square of the shell thickness (Figure 10), which is reasonable, as the stiffness shows the same dependence.[17] This relation explains the "floppy" appearance of thin shells on SEM pictures. Shells thinner than 15 nm can be irreversibly deformed even by capillary forces during drying, whereas the surface of thick shells can be locally damaged by the tip before buckling occurs. A spherical shell loses its shape when the work done by the external pressure equals the deformation energy.[31,32] The critical value is usually considered the force required for an impression by a distance equal to the shell thickness. Hence, it

(30) Oliver, W. C.; Pharr, G. M. *J. Mater. Res.* **1992**, *7*, 1564.

(31) Gao, C.; Donath, E.; Moya, S.; Dudnik, V.; Möhwald, H. *Eur. Phys. J. E* **2001**, *5*, 21.

(32) Pogorelov, A. V. *Bending of Surfaces and Stability of Shells*; American Mathematical Society: Providence, RI, 1988; Vol. *iii*, p 77.

should also depend on the diameter of the sphere. Interestingly, we did not detect any such dependence in our experiments. It remains to be clarified whether this is due to the experimental uncertainty in defining the onset of buckling.

V. Conclusion

Using PS spheres of different size as templates, we synthesized hollow silica spheres whose shell thickness could be sensitively tuned by modifying the reaction conditions.

By applying a point load via a sharp AFM tip and recording force−distance curves, we directly investigated their mechanical properties. Within the linear elastic regime, i.e., at small loading forces, the elastic modulus of the shells was determined to be largely independent of shell thickness and sphere size within the studied size range. Hence, even shells as thin as 15 nm behave in the same way as bulk silica particles obtained by the same synthesis procedure. That heat treatment at 850 °C raises the slope of the elastic response indicates that incomplete condensation of the siloxane backbone structure is responsible for the lower elastic modulus found in our silica particles. At higher force load, we also observed buckling of the shells. In accordance with expectations, the force required for buckling was found to be proportional to the square of the shell thickness. As the applied point forces correspond to approximately 10^8-10^9 Pa, the hollow silica spheres proved extremely stable toward elastic as well as plastic shell deformation by point force loads.

Acknowledgment. We are grateful to G. Schäfer for helping with the synthesis, M. Müller for taking the SEM images, K. Kichhoff for taking the TEM images, H.-J. Butt, A. Imhof, and A. Fery for useful discussion, and B. Ullrich for carefully reading the manuscript. D.V. and G.K.A. acknowledge support by the German Science Foundation via SFB TR6 and MdA via SPP 1273. A.v.B. acknowledges the Stichting voor Fundamental Onderzoek der Materie (FOM), which is supported by the Nederlandse Organisatie voor Wetenschappelijk Onderzoek (NWO).

LA803546R